Defense Technical Information Center Compilation Part Notice

ADP016735

TITLE: Theory and Computation of Multilayer Composites

DISTRIBUTION: Approved for public release, distribution unlimited
NATO

This paper is part of the following report:

TITLE: Mechanics of Composite Materials and Structures. Volume 2: Main Lectures

To order the complete compilation report, use: ADA428068

The following component part numbers comprise the compilation report:
ADP016731 thru ADP016748

THEORY AND COMPUTATION OF MULTILAYER COMPOSITES

E. STEIN AND J. TESSMER
Institute for Structural Mechanics and Computational Mechanics, University of Hannover, Appelstraße 9A, D-30167 Hannover, Germany

Abstract. An hierarchical concept for the analysis of thin-walled composite shells is presented within the finite element method for nonlinear deformation of thin-walled composite structures. For non-disturbed subdomains of the structure an effective 4-node shell element with 5 or 6 d.o.f. per node is used for the whole laminate. For the analysis of 3D-stress states a multidirector shell element along the thickness with piecewise polynomials is presented. n physical layers are approximated by N numerical layers, discretized with hierarchical trial- and test functions. The coupling of both elements is performed by special transition elements. An example shows the technique and efficiency of coupling both types of elements.

1. Introduction

Composites are typically used for light-weight structures, and in many engineering fields there are attempts to replace components with classical materials (steel, concrete) by fiber reinforced materials. Therefore we focus on the computation of thin-walled laminated composites. Due to anisotropy and inhomogenity these structures show rather complicated states of stresses and strains such that several adequate mechanical models for thin composite structures have been developed in recent years, see [5, 9].

Different FE-methods were applied with respect to special purposes (global deformation analysis, stress analysis, first ply failure criteria, local stress singularities, crack analysis), see e.g. [2, 8]. By admitting a priori delaminations between plies and regarding their growth, load depending disturbances of the perfect geometry of cross-sections are growing and diminish the critical load within stability analysis. We present an hierarchical

multi-layer shell model as a framework for the efficient nonlinear analysis of delamination and failure process, focusing on basic topics of composite theory and computation. In [10] the failure analysis for this model is shown. For calculating a complete 3D stress state in disturbed subdomains a multidirector shell kinematic with deformation modes in thickness direction is used and implemented in FEM. Within this kinematics, the interpolation in thickness direction with hierarchical polynomials per layer is independent from in plane interpolation. Since dominant parts of composite shells usually reside in 2D stress states with little transvere shear deformation, a conventional Reissner-Mindlin kinematic is used for regular parts. In these areas normal stresses S^{33} are much smaller than normal in-plane stresses. Therefore, S^{33} is neglected in the classical laminate theory. For coupling both kinematic types within a finite element method a transition element is applied.

2. Kinematics

The considered thin-walled composite structures consist of a layerwise build up with n physical layers j of thickness h^j and N numerical layers i which can collect or subdivide the physical layers for numerical calculations, fig. 1 and 2

The position vector $\mathbf{X}_0$ of the reference surface S_0 is parametrizised by convected coordinates Θ^α. An orthonormal basis system $\mathbf{t}_k(\Theta^\alpha)$ is attached to this surface where $\mathbf{t}_3$ is a normal vector and Θ^3 the coordinate in thickness direction. The transformation between the different base systems is given by $\mathbf{t}_k(\Theta^\alpha) = \mathbf{R}_0(\Theta^\alpha)\,\mathbf{e}_k$ where $\mathbf{R}_0$ is a proper orthogonal tensor.

Depending on the desired accuracy and numerical effort two different types of kinematics are applied. One is the standard shell kinematic with one director, yielding a 2D-FE-formulation with 5 or 6 d.o.f. per node, and the other is a 3D-multi-director kinematic which still yields a 2D-like finite element data structure by a priori C^0-continuous hierarchical shape functions in thickness direction, such we get the numerical complexity of a 3D-brick formulation.

2.1. INEXTENSIBLE ONE-DIRECTOR KINEMATICS

The position vectors of the reference and the current configuration of the shell body are given by

$$\begin{aligned} \mathbf{X}(\Theta^\alpha,\Theta^3) &= \mathbf{X}_0(\Theta^\alpha) + \Theta^3\,\mathbf{t}_3(\Theta^\alpha)\,, \quad -h_u \le \Theta^3 \le h_o\,, \\ \mathbf{x}(\Theta^\alpha,\Theta^3) &= \mathbf{x}_0(\Theta^\alpha) + \Theta^3\,\mathbf{d}(\Theta^\alpha)\,, \end{aligned} \tag{1}$$

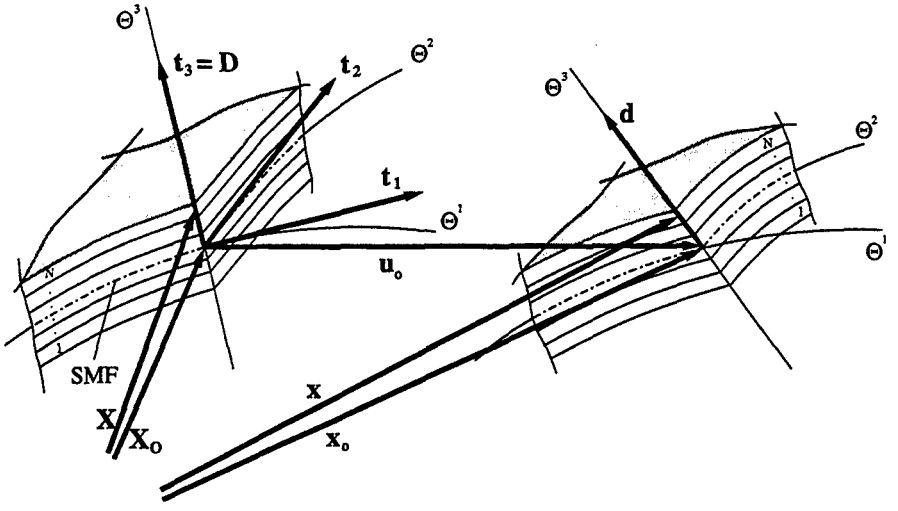

Figure 1. One-Director-Kinematic

$$\begin{aligned} \text{with} \quad \mathbf{x}_0(\Theta^\alpha) &= \mathbf{X}_0(\Theta^\alpha) + \mathbf{u}_0(\Theta^\alpha)\,, \\ \mathbf{d} &= \mathbf{a}_3 = \mathbf{R}\,\mathbf{t}_3\,, \quad \|\mathbf{d}\| = \|\mathbf{t}_3\| = 1\,, \\ \mathbf{R} &= f(\Delta\boldsymbol{\beta}) \in SO^3\,, \quad \Delta\boldsymbol{\beta} = \text{rotational vector}\,, \\ \mathbf{v} &= [\mathbf{u}_0; \Delta\boldsymbol{\beta}]^T\,. \end{aligned} \tag{2}$$

$\mathbf{u}_0$ is the displacement vector of the reference surface, $\mathbf{d}$ the director vector, and $\mathbf{R}$ is an orthogonal tensor generated by application of the Euler-Rodriguez-formula on the rotational vector $\Delta\boldsymbol{\beta}$, see e.g. [1].

The Green-Lagrangian strain tensor $\mathbf{E} = E_{ij}\mathbf{G}^i \otimes \mathbf{G}^j$ is formulated with respect to the tangential base vectors $\mathbf{G}_k = \mathbf{X}_{,k} = \partial\mathbf{X}/\partial\Theta^k$ for the inextensible thinwalled structure.

$$E_{ij} = \tfrac{1}{2}(\mathbf{x}_{,i}\,\mathbf{x}_{,j} - \mathbf{X}_{,i}\,\mathbf{X}_{,j}) = \varepsilon_{ij} + \kappa_{ij}\Theta^3 + |\,...(\Theta^3)^2\,, \tag{3}$$

with the approximations

$$\begin{aligned} \varepsilon_{\alpha\beta} &= 0.5(\mathbf{x}_{,\alpha}\,\mathbf{x}_{,\beta} - \mathbf{X}_{,\alpha}\,\mathbf{X}_{,\beta})\,, \\ \gamma_\alpha &= 2\varepsilon_{\alpha 3} = (\mathbf{x}_{0,\alpha}\cdot\mathbf{d} - \mathbf{X}_{0,\alpha}\cdot\mathbf{t}_3)\,, \\ \kappa_{\alpha\beta} &= 0.5[(\mathbf{x}_{0,\alpha}\cdot\mathbf{d}_{,\beta} + \mathbf{d}_{,\alpha}\cdot\mathbf{x}_{0,\beta}) - (\mathbf{X}_{0,\alpha}\cdot\mathbf{t}_{3,\beta} + \mathbf{t}_{3,\alpha}\cdot\mathbf{X}_{0,\beta})]\,. \end{aligned} \tag{4}$$

2.2. EXTENSIBLE MULTIDIRECTOR KINEMATICS

For the description of 3D-stress-states an extended multidirector kinematic is used. The position vectors of the reference and the current configuration of the shell body are given by

$$\begin{aligned} \mathbf{X}(\Theta^\alpha, \Theta^3) &= \mathbf{X}_0(\Theta^\alpha) + \Theta^3\,\mathbf{t}_3(\Theta^\alpha) \quad -h_u \le \Theta^3 \le h_o\,, \\ \mathbf{x}(\Theta^\alpha, \Theta^3) &= \mathbf{X}(\Theta^\alpha, \Theta^3) + \mathbf{u}(\Theta^\alpha, \Theta^3)\,. \end{aligned} \tag{5}$$

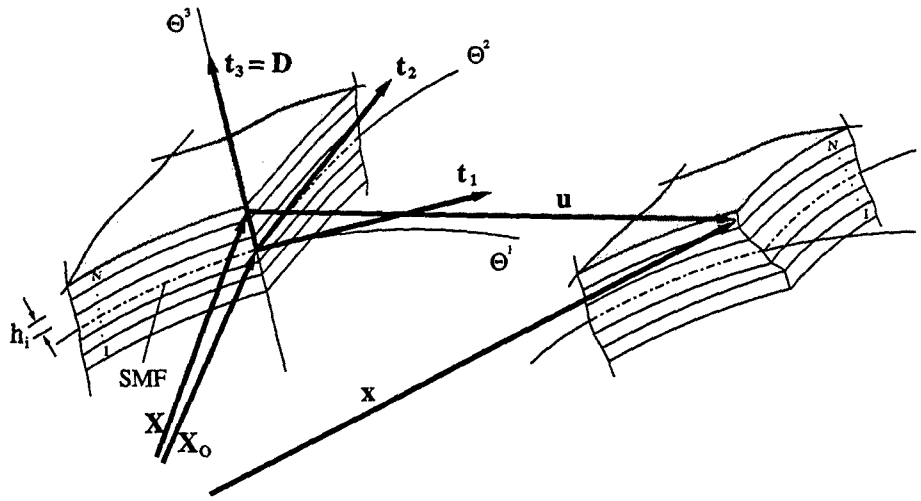

Figure 2. Multi-Director-Kinematic for N numerical layers

A multiplicative decomposition of $\mathbf{u}$ is introduced as

$$\begin{aligned}
\mathbf{u}(\Theta^\alpha, \Theta^3) &= \sum_{l=1}^{k} \bar{\mathbf{u}}_l(\Theta^\alpha)\, w_l(\Theta^3) = \mathbf{\Phi}(\Theta^3)\, \bar{\mathbf{u}}(\Theta^\alpha)\,, \\
\bar{\mathbf{u}}(\Theta^\alpha) &= [\underbrace{\bar{\mathbf{u}}_1, \bar{\mathbf{u}}_2, \dots, \bar{\mathbf{u}}_m}_{\bar{\mathbf{u}}^1 \text{ (layer 1)}}, \dots, \underbrace{\bar{\mathbf{u}}_{s+1}, \bar{\mathbf{u}}_{s+2}, \dots, \bar{\mathbf{u}}_{s+m}}_{\bar{\mathbf{u}}^i \text{ (layer } i)}, \dots, \bar{\mathbf{u}}_{N(m-1)+1}]^T
\end{aligned} \tag{6}$$

where k is the number of interpolation points over the thickness, w_l are shape function (piecewise linear for $k = N+1$), $s = (i-1)\,(m-1)$ is a layer index, and m is the polynomial degree, $(2 \le m \le 4)$. In thickness direction hierarchical shape functions are defined for each numerical layer i as $\mathbf{\Phi}^i(\Theta^3)$.

$$\begin{aligned}
&\mathbf{u}^i(\Theta^\alpha, \Theta^3) = \mathbf{\Phi}^i(\Theta^3)\, \bar{\mathbf{u}}^i(\Theta^\alpha)\,, \qquad \bar{\mathbf{u}}^i(\Theta^\alpha) = [\bar{\mathbf{u}}^i_1, \bar{\mathbf{u}}^i_2, \quad \dots \quad, \bar{\mathbf{u}}^i_m]^T\,, \\
&\bar{\mathbf{u}}^i_1 = [\bar{u^i_{1x}}, \bar{u^i_{1y}}, \bar{u^i_{1z}}]^T\,, \qquad \mathbf{\Phi}^i(\Theta^3) = [\phi^i_1\mathbf{1}, \phi^i_2\mathbf{1}, \quad \dots \quad, \phi^i_m\mathbf{1}]\,, \\
&\phi^i_1(\zeta^i) = 0.5(1-\zeta^i)\,, \quad \phi^i_3(\zeta^i) = 1-\zeta^{i2}\,, \quad \zeta^i = 2\,\Theta^3/h^i \\
&\phi^i_2(\zeta^i) = 0.5(1+\zeta^i)\,, \quad \phi^i_4(\zeta^i) = (1-\zeta^{i2})\zeta^i\,.
\end{aligned} \tag{7}$$

This leads to an a priori discretization in thickness direction within the analytical shell theory, analogous to the analytical thickness integration of stress resultants in classical shell models. These shape functions are independent from the in-plane trial-functions, see sec. 5.2. For linear plates see [8, 9]. A layerwise linear interpolation is realized by using ϕ^i_1 and ϕ^i_2 only.

In contrast to eq.(4) the Green-Lagrangian strain tensor is computed and applied in its complete form , eq.(3).

3. Material Equations on Macro Level

3D-material equations are formulated for each physical layer of the composite laminate . These have to be transformed from the fiberoriented basis to the local basis of the shell, see [5]. In case of standard shell kinematics they are integrated a priori over the thickness of the overall thickness.

3.1. UNI-DIRECTIONAL TRANSVERSAL ISOTROPIC LAYERS

The constitutive equations for unidirectional (UD) layers of laminated structures are derived under the assumption of small strains and the validity of St. Venant Kirchhoff material equations with linearized strains.

Hence, the free energy $\bar{W}(\mathbf{E}) = \frac{1}{2}\mathbf{E} \cdot \mathbb{C}\mathbf{E}$ is formulated as a quadratic function of $\mathbf{E}$. The material tensor $\mathbb{C}$ is constant with respect to the invariants $\mathrm{tr}\mathbf{E}$, $\mathrm{tr}(\mathbf{E}^2)$, $\mathbf{a}_0 \cdot \mathbf{E}\mathbf{a}_0$, $\mathbf{a}_0 \cdot \mathbf{E}^2\mathbf{a}_0$. Using the elastic parameters $\lambda, \mu_T, \mu_L, \alpha, \beta$, the free energy $\bar{W}$, the stresses $\mathbf{S}$ and the constant material tensor $\mathbb{C}$ follow as

$$\begin{aligned} \bar{W}(\mathbf{E}) &= \tfrac{1}{2}\lambda(\mathrm{tr}\mathbf{E})^2 + \mu_T \mathrm{tr}(\mathbf{E}^2) + \alpha(\mathbf{a}_0 \cdot \mathbf{E}\mathbf{a}_0)\mathrm{tr}\mathbf{E} \\ &\quad +2(\mu_L - \mu_T)(\mathbf{a}_0 \cdot \mathbf{E}^2\mathbf{a}_0) + \tfrac{1}{2}\beta(\mathbf{a}_0 \cdot \mathbf{E}\mathbf{a}_0)^2, \\ \text{with} \qquad \mathbf{S} &= \frac{\partial \bar{W}(\mathbf{E})}{\partial \mathbf{E}} = \mathbb{C} \cdot \mathbf{E}\,, \quad \mathbb{C} = \frac{\partial^2 \bar{W}(\mathbf{E})}{\partial \mathbf{E}^2}\,. \end{aligned} \tag{8}$$

For UD-layers with the fiber direction $\mathbf{a}_0 = \mathbf{e}_1 = (1,0,0)$ and by computation of $\mathbb{C}\mathbb{C}^{-1} = \mathbf{1}$ the components of the compliance matrix $\mathbb{C}^{-1}$ result with the common elasticity constants in

$$\mathbb{C}^{-1} = \begin{bmatrix} 1/E_1 & -\nu_{12}/E_1 & -\nu_{12}/E_1 & 0 & 0 & 0 \\ -\nu_{12}/E_1 & 1/E_2 & -\nu_{23}/E_2 & 0 & 0 & 0 \\ -\nu_{12}/E_1 & -\nu_{23}/E_2 & 1/E_2 & 0 & 0 & 0 \\ 0 & 0 & 0 & 1/G_{12} & 0 & 0 \\ 0 & 0 & 0 & 0 & 1/G_{12} & 0 \\ 0 & 0 & 0 & 0 & 0 & 1/G_{23} \end{bmatrix}. \tag{9}$$

3.2. HYPERELASTIC ISOTROPIC INTERMEDIATE LAYERS

For composite structures with macroscopicly seperated parts of anisotropic and isotropic material, e.g. tires, also a hyperelastic isotropic material equation is formulated with respect to the invariants of the Cauchy-Green tensor $\mathbf{C} = \mathbf{F}^T\mathbf{F} = 2\mathbf{E} + \mathbf{1}$. The stored energy by 'Blatz & Ko', [7], yields

$$\begin{aligned} W &= \frac{1}{2}\mu_0[f(J_1 - 3) + (1-f)(J_2 - 3) + \\ &\qquad \left(\frac{1-2\nu_0}{\nu_0}\right)\{f(J_3^{\frac{-2\nu_0}{1-2\nu_0}} - 1) + (1-f)(J_3^{\frac{2\nu_0}{1-2\nu_0}} - 1)\}], \end{aligned} \tag{10}$$

$$\text{with} \quad J_1 = I_1\,, \quad J_2 = I_2/I_3\,, \quad J_3 = \sqrt{I_3} = J\,;$$
$$I_1 = \mathrm{tr}\mathbf{C}\,, \quad I_2 = 0.5[(\mathrm{tr}\mathbf{C})^2 - \mathrm{tr}\mathbf{C}^2]\,, \quad I_3 = \det\mathbf{C}\,.$$

The 2. Piola-stress tensor $\mathbf{S}$ and the material tensor $\mathbb{C}$ follow as

$$\begin{aligned} \mathbf{S} &= \frac{\partial W}{\partial \mathbf{E}_2} = 2\frac{\partial}{\partial \mathbf{C}} W(I_1(\mathbf{C}), I_2(\mathbf{C}), I_3(\mathbf{C}))\,, \\ \mathbb{C} &= 4\frac{\partial^2}{\partial \mathbf{C}^2} W(I_1(\mathbf{C}), I_2(\mathbf{C}), I_3(\mathbf{C})). \end{aligned} \tag{11}$$

$$\begin{aligned} \Longrightarrow \quad \mathbf{S} &= \mu_0[f + \frac{I_1}{J^2}(1-f)]\mathbf{1} - \frac{\mu_0}{J^2}(1-f)\mathbf{C} + \mu_0\beta_1\mathbf{C}^{-1}\,, \\ \mathbb{C} &= 2\frac{\mu_0}{J^2}(1-f)(\mathbf{1}\otimes\mathbf{1} - \mathbb{I}) + 2\mu_0\beta_1\frac{\partial \mathbf{C}^{-1}}{\partial \mathbf{C}} \\ &\quad + [\mu_0\frac{2\nu_0}{1-2\nu_0}\beta_2 + 2\mu_0\frac{I_2}{J^2}(1-f)]\mathbf{C}^{-1}\otimes\mathbf{C}^{-1} \\ &\quad + 2\frac{\mu_0}{J^2}(1-f)(\mathbf{C}^{-1}\otimes\mathbf{C} + \mathbf{C}\otimes\mathbf{C}^{-1}) \\ &\quad - 2I_1\frac{\mu_0}{J^2}(1-f)(\mathbf{C}^{-1}\otimes\mathbf{1} + \mathbf{1}\otimes\mathbf{C}^{-1})\,, \end{aligned} \tag{12}$$

$$\begin{aligned} \text{with} \quad \beta_1 &= -fJ^{\frac{-2\nu_0}{1-2\nu_0}} + (1-f)J^{\frac{2\nu_0}{1-2\nu_0}} - J_2(1-f)\,, \\ \beta_2 &= fJ^{\frac{-2\nu_0}{1-2\nu_0}} + (1-f)J^{\frac{2\nu_0}{1-2\nu_0}}\,, \\ \frac{\partial \mathbf{C}^{-1}}{\partial \mathbf{C}} &= -\mathbf{C}^{-1}\mathbb{I}\mathbf{C}^{-1}. \end{aligned}$$

3.3. RESULTANT FORMULATION FOR ONE-DIRECTOR SHELL

Since the material equations for one-director shells are formulated in resultants of stresses and strains, an adequate transformation and integration of the material law, eq.(9), is conducted. With the assumption of $S^{33} = 0$ the matrix $\mathbb{C}_{6\times6}$ can be statically kondensed to $\mathbb{C}^R_{5\times5}$. Such, we get for the fiberorientated basis

$$\mathbf{S}^R_F = \mathbb{C}^R_F\,\mathbf{E}^R_F \quad \text{with} \quad \mathbb{C}^R_F = \begin{bmatrix} \mathbb{C}^F_m & \mathbf{0} \\ \mathbf{0} & \mathbb{C}^F_s \end{bmatrix},$$

$$\begin{aligned} &C^F_{m11} = E_1/(1-\nu^2\tfrac{E_2}{E_1})\,, \quad C^F_{m13} = 0\,, \quad C^F_{s11} = G_{12}\,, \\ &C^F_{m12} = E_2\nu/(1-\nu^2\tfrac{E_2}{E_1})\,, \quad C^F_{m23} = 0\,, \quad C^F_{s12} = 0\,, \\ &C^F_{m22} = E_2/(1-\nu^2\tfrac{E_2}{E_1})\,, \quad C^F_{m33} = G_{12}\,, \quad C^F_{s22} = G_{23} \end{aligned} \tag{13}$$

$$\mathbf{S}^R = \left[S^{11}; S^{22}; S^{12}; S^{13}; S^{23}\right]\,, \quad \mathbf{E}^R = [E_{11}; E_{22}; 2E_{12}; 2E_{13}; 2E_{23}]\,.$$

For the integration over the thickness all matrices for each layer j must be transformed to the local basis of the reference surface, see [4].

$$\mathbb{C}^{jR}_L = \bar{\mathbf{T}}^{jT}\mathbb{C}^R_F\bar{\mathbf{T}}^j = \begin{bmatrix} \mathbb{C}^j_m & \mathbf{0} \\ \mathbf{0} & \mathbb{C}^j_s \end{bmatrix} \tag{14}$$

$$\Longrightarrow \quad \hat{\mathbf{S}} = \hat{\mathbb{C}} \cdot \hat{\mathbf{E}} = \begin{bmatrix} \mathbf{N} \\ \mathbf{M} \\ \mathbf{Q} \end{bmatrix} = \begin{bmatrix} \mathbf{D}_m & \mathbf{D}_{mb} & \mathbf{0} \\ \mathbf{D}_{mb}^T & \mathbf{D}_b & \mathbf{0} \\ \mathbf{0} & \mathbf{0} & \mathbf{D}_s \end{bmatrix} \cdot \begin{bmatrix} \boldsymbol{\varepsilon} \\ \boldsymbol{\kappa} \\ \boldsymbol{\gamma} \end{bmatrix}, \tag{15}$$

$$\begin{aligned} \text{with} \quad \hat{\mathbf{S}} &= [N^{11}; N^{22}; N^{12}; M^{11}; M^{22}; M^{12}; Q^1; Q^2]^T, \\ \hat{\mathbf{E}} &= [\varepsilon_{11}; \varepsilon_{22}; 2\varepsilon_{12}; \kappa_{11}; \kappa_{22}; 2\kappa_{12}; \gamma_1; \gamma_2]^T \\ \mathbf{D}_m &= \textstyle\sum_j \mathbb{C}_m^j h^j, \qquad \mathbf{D}_{mb} = \sum_j \mathbb{C}_m^j (z_s h)^j, \\ \mathbf{D}_b &= \textstyle\sum_j \mathbb{C}_m^j (z_s^2 h + \frac{h^3}{12})^j, \qquad \mathbf{D}_s = \sum_j \mathbb{C}_s^j h^j \end{aligned}$$

4. Variational Equations

In this section the weak form of equilibrium (principle of virtual work) is given. Linearization yields the consistent tangential operator.

4.1. ONE-DIRECTOR FORMULATION

The principle of virtual work is given in the material description for the inextensible shell in thickness direction and external loads $\hat{\mathbf{t}}$ at the reference surface, using (15)

$$\begin{aligned} G(\mathbf{u}, \boldsymbol{\eta}) &= \int_{(V)} \mathbf{S} \cdot \delta \mathbf{E} \, dV - \int_{(\Gamma_\sigma)} \hat{\mathbf{t}} \cdot \boldsymbol{\eta} \, d\Gamma_\sigma = 0 \\ &= \int_{(\Omega)} (N^{\alpha\beta} \delta\varepsilon_{\alpha\beta} + M^{\alpha\beta} \delta\kappa_{\alpha\beta} + Q^\alpha \delta\gamma_\alpha) d\Omega \; - \; G_{ext}(\hat{\mathbf{t}}, \boldsymbol{\eta}) \\ &= \int_{(\Omega)} \hat{\mathbf{S}} \cdot \delta\hat{\mathbf{E}} \, d\Omega \; - \; G_{ext}(\hat{\mathbf{t}}, \boldsymbol{\eta}) \, . \end{aligned} \tag{16}$$

For constant material matrix $\hat{\mathbb{C}}$ and conservative loads the linearization (Gâteaux-derivative) of (16) yields

$$DG(\mathbf{u}, \boldsymbol{\eta}) \cdot \Delta\mathbf{u} = \int_{(\Omega)} \delta\hat{\mathbf{E}} \cdot \hat{\mathbb{C}} \cdot \Delta\hat{\mathbf{E}} \, d\Omega + \int_{(\Omega)} \hat{\mathbf{S}} \Delta\delta\hat{\mathbf{E}} \, d\Omega \, . \tag{17}$$

4.2. MULTIDIRECTOR FORMULATION

The laminate structure is loaded at the bottom- and top-surface Ω_σ with $\hat{\mathbf{p}} = \hat{p}^k \, \mathbf{e}_k$. Hence, the virtual work reads in index notation

$$G(\mathbf{u}, \boldsymbol{\eta}) = \int_{(\Omega)} [\int_{(\Theta^3)} S^{kl} \, \delta E_{kl} \, J d\Theta^3] \, d\Theta^2 d\Theta^1 - \int_{(\Omega_\sigma)} \hat{p}^k \, \eta_k \, d\Omega_\sigma = 0 \, , \tag{18}$$

with $J(\Theta^i) = (\mathbf{X}_{,1} \times \mathbf{X}_{,2}) \cdot \mathbf{X}_{,3}$. Note the special splitting of the volume integral in two parts. Through this split it is possible to apply the same interpolation functions with respect to the reference surface for the multi-director formulation and for the one-director kinematics. Linearization yields

$$DG(\mathbf{u}, \boldsymbol{\eta}) \cdot \Delta\mathbf{u} = \int_{(\Omega)} [\int_{(\Theta^3)} (\delta E_{kl} C^{klmn} \Delta E_{mn} + S^{kl} \Delta\delta E_{kl}) \, J d\Theta^3] \, d\Omega \, . \tag{19}$$

5. Finite Element Discretization

The four node quadrilateral Q1-element with isoparametric bilinear shape functions is used in the reference surface for all kinematic quantities. For one-director kinematic shell elements with 5 or 6 d.o.f. per node and for multi-director kinematics shell elements with more than 6 d.o.f. per node are applied. For coupling both types of finite elements a special transition element is used.

5.1. ONE-DIRECTOR ELEMENT

The approximation of geometry and displacements reads

$$\mathbf{X}_{0_h} = \sum_{K=1}^{4} N_K(\xi,\eta)\,\mathbf{X}_{0K}\,, \quad \text{and} \quad \mathbf{v}_h = \sum_{K=1}^{4} N_K(\xi,\eta)\,\mathbf{v}_K\,, \tag{20}$$

where $\mathbf{v}_K = [\mathbf{u}_0; \Delta\boldsymbol{\beta}]_K^T$ is the nodal displacement vector; it consists of the displacement components of the reference surface and the increment of the rotational vector. Depending on the place of the node (within flat areas or at intersections) the rotational vector is parametrisized with respect to the local basis (5 d.o.f.) or the global basis (6 d.o.f.). Following eqs.(1)-(3), all necessary kinematic values are computed. With the differential operator matrix $\mathbf{B}$, see [5], we get

$$[\ \delta\boldsymbol{\epsilon}\,,\ \delta\boldsymbol{\kappa}\,,\ \delta\tilde{\boldsymbol{\gamma}}\ ]^T = \sum_{K=1}^{4} \mathbf{B}_K\,\delta\mathbf{v}_K\,. \tag{21}$$

Applying the virtual work principle (16) and linearization (17) yields

$$\begin{aligned} &G(\mathbf{v},\delta\mathbf{v}) = \sum_{K=1}^{4} \delta\mathbf{v}_K^T\,\mathbf{G}_K\,, \quad \text{with } \mathbf{G}_K = \int_{\Omega_e} (\mathbf{B}_K^T\hat{\mathbf{S}} - N_K\hat{\mathbf{t}})\,d\Omega\,, \\ &D\mathbf{G}(\mathbf{v},\delta\mathbf{v})\Delta\mathbf{v} = \sum_{K=1}^{4}\sum_{L=1}^{4} \delta\mathbf{v}_K^T\mathbf{K}_{KL}\Delta\mathbf{v}_L\,, \\ &\text{with } \mathbf{K}_{KL} = \int_{\Omega_e} (\mathbf{B}_K^T\hat{\mathbf{C}}\mathbf{B}_L + \mathbf{G}_{KL})\,d\Omega\,. \end{aligned} \tag{22}$$

5.2. MULTIDIRECTOR ELEMENT

One major advantage of the multi director formulation in contrast to a standard 3D-finite element is the 2D-data structure with bilinear shape functions with respect to the reference surface, which allows for an easy coupling with standard shell elements. The approximation of the geometry and the displacement field of layer i, eqs. (7)-(5), follows from

$$\begin{aligned} \mathbf{X}_h &= \sum_{K=1}^{4} N_K(\xi,\eta)\,\mathbf{X}_K\,, \qquad \mathbf{X}_{K_h} = \mathbf{X}_{0K} + \Theta^3\,\mathbf{t}_{3K}\,, \\ \mathbf{u}_h^i &= \sum_{K=1}^{4} N_K(\xi,\eta)\boldsymbol{\Phi}^i\,\mathbf{u}_K. \end{aligned} \tag{23}$$

The number of components for $\mathbf{u}_K$ is $3(N+1)+3N(m-2)$. Again, with the differential operator $\mathbf{B}$-matrix, see [4], $\delta\mathbf{E} = \sum_{K=1}^{4} \mathbf{B}_K\,\delta\mathbf{u}_K$. Putting into (18) and (19) yields

$$
\begin{aligned}
&G(\mathbf{u},\boldsymbol{\eta}) = \sum_{K=1}^{4} \delta\mathbf{u}_K^T\,\mathbf{G}_K\,,\\
&\text{with } \mathbf{G}_K = \int_{(\Omega_e)} [\sum_{j=1}^{n} \int_{(\Theta^3)} \mathbf{B}_K^T\,\mathbf{S} J \frac{h^j}{2} d\,\zeta^j]\,d\Omega_e - \int_{(\Omega_{e\sigma})} N_K \hat{\mathbf{p}} \bar{J}\,d\Omega_{e\sigma}\,,\\
&D\mathbf{G}(\mathbf{u},\boldsymbol{\eta})\Delta\mathbf{u} = \sum_{K=1}^{nel}\sum_{L=1}^{nel} \delta\mathbf{u}_K^T\,\mathbf{K}_{KL}\,\Delta\mathbf{u}_L\,,\\
&\text{with } \mathbf{K}_{KL} = \int_{(\Omega_e)} \sum_{j=1}^{n} \int_{(\Theta^3)} (\mathbf{B}_K^T\,\mathbb{C}^j\,\mathbf{B}_L + \mathbf{G}_{KL}^j)\,J\frac{h^j}{2} d\zeta^j\,d\Omega_e\,.
\end{aligned}
\tag{24}
$$

5.3. TRANSITION ELEMENT

For coupling standard one-director with multi-dirctor shells a transition element is used. To prevent sensible disturbances of the 3D-stress state each layer i has to be allowed for a constant thickness strains E_{33}^i at the multi-director side of the transition element and C^0–continuity only in the mid-surface at the other one-director side, see [6]. Such a thickness jump of the deformed laminate is admitted there.

5.4. SHEAR-LOCKING

All presented elements use a special interpolation of transverse shear strains to prevent "shear-locking", namely an assumed natural strain (ANS) method, see [3],

$$
\tilde{\gamma} = \begin{bmatrix} \gamma_\xi \\ \gamma_\eta \end{bmatrix} = \frac{1}{2} \begin{bmatrix} (1-\eta)\gamma_{\xi B} & + & (1+\eta)\gamma_{\xi D} \\ (1-\xi)\gamma_{\eta A} & + & (1+\xi)\gamma_{\eta C} \end{bmatrix}. \tag{25}
$$

In this formulation shear strains in the mid-side nodes ($M = A, B, C, D$) are computed by the standard bilinear shape functions $N_K(\xi,\eta)$ of the element.

6. Example

Steel-Cord-Reinforced Rubber Beam under vertical load.
Cross-sec.: width/height = 100/20; Layersequenz [iso/20°/iso/ − 20°/iso].

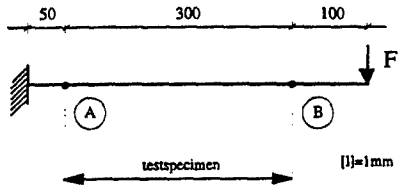

Figure 3. Composite-Beam

Element	Equat.	CPU
1. One-Dir.-Shell	720	1.3
2. Multi-Dir.-Shell, N=15	6912	135.5
3. Coupling 1. and 2. in A and B	2925	39.8

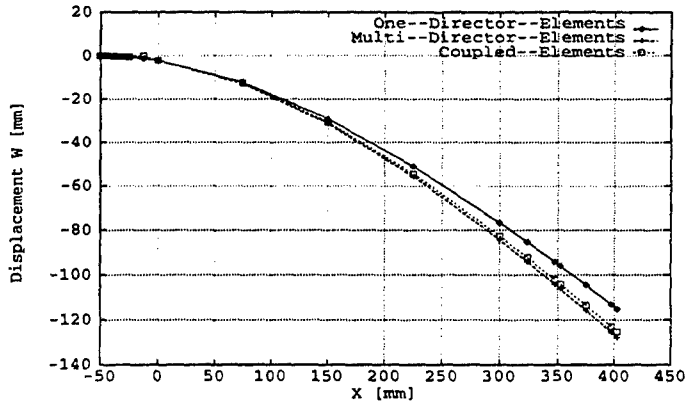

Figure 4. Displacement curves

References

1. Betsch, P., Menzel, A., and Stein, E. (1998) On the Parametrization of Finite Rotations in Computational Mechanics. A Classification of Concepts with Application to Smooth Shells, *Comp. Meth. Appl. Mech. Engrg.*, **155**, 273–305.
2. Cochelin, B., Damil, N., and Potier-Ferry, M. (1994) Asymptotic-numerical methods and pade approximants for non-linear elastic structures, *Int. J. for Numerical Meth. in Engrg.*, **37**, 1137–1213.
3. Dvorkin, E. and Bathe, K.-J. (1984) A Continuum Mechanics Based Four-Node Shell Element for General Nonlinear Analysis, *Eng. Comput.*, 1, 77–88.
4. Gruttmann, F. (1996), *Theorie und Numerik dünnwandiger Faserverbundstrukturen*, Habilitation, Bericht-Nr. F 96/1, Institut für Baumechanik und Numerische Mechanik der Universität Hannover.
5. Gruttmann, F. and Wagner, W. (1994) On the numerical analysis of local effects in composite structures, *Composite Structures*, **29**, 1–12.
6. Gruttmann, F. and Wagner, W. (1996) Coupling of 2D- and 3D-composite shell elements in linear and nonlinear applications, *Comput. Methods Appl. Mech. Engrg.*, **129**, 271–278.
7. Levinson, M. and Burgess, I. (1971) A comparison of some simple constitutive relations for slightly compressible rubber-like materials, *Int. J. Mech. Sci.*, **13**, 563–572.
8. Reddy, J. (1987) Generalization of two-dimensional theories of laminated composite plates, *Communications in Applied Numerical Methods*, **3**, 173–180.
9. Robbins, D. and Reddy, J. (1993) Modeling of thick composites using a layerwise laminate theory, *Int. J. Numer. Methods Eng.*, **36**, 655–677.
10. Stein, E. and Teßmer, J. (1998) Theory and Computation of Damage and Failure of Composites, in C. A. Mota Soares (ed.), *NATO ASI on Mechanics of Composite Materials and Structures*, Kluwer, Dordrecht.